Journal of
Synchrotron Radiation

ISSN 0909-0495

Received 5 February 2008
Accepted 2 May 2008

On the use of clessidra prism arrays in long-focal-length X-ray focusing

Werner Jark,* Marco Matteucci and Ralf Hendrik Menk

Sincrotrone Trieste ScpA, SS 14 km 163.5, 34012 Basovizza (TS), Italy.
E-mail: werner.jark@elettra.trieste.it

Clessidra (hour-glass) X-ray lenses have an overall shape of an old hour glass, in which two opposing larger triangular prisms are formed of smaller identical prisms or prism-like objects. In these lenses, absorbing and otherwise optically inactive material was removed with a material-removal strategy similar to that used by Fresnel in the lighthouse lens construction. It is verified that when the single prism rows are incoherently illuminated they can be operated as independent micro-lenses with coinciding image positions for efficient X-ray beam concentration. Experimental data for the line width and the refraction efficiency in one-dimensional focusing are consistent with the expectations. Imperfections in the structures produced by state-of-the-art deep X-ray lithography directed only 35% of the incident intensity away from the image and widened it by just 10% to 125 μm. An array of micro-lenses with easily feasible prism sizes is proposed as an efficient retrofit for the refocusing optics in an existing beamline, where it would provide seven-fold flux enhancement.

© 2008 International Union of Crystallography
Printed in Singapore – all rights reserved

Keywords: X-ray optics; refraction; deep X-ray lithography; kinoform lens.

1. Introduction

From the optical point of view the regular clessidra prism array shown in Fig. 1 presents a kinoform (Lesem *et al.*, 1969) or Fresnel (Yang, 1993) transmission lens for the focusing of X-rays in the vertical direction. The optimization of the properties of such a lens for one-dimensional focusing is discussed by Jark *et al.* (2006). The conditions required for obtaining the smallest possible line width by use of these optical components are spatially coherent illumination of the whole aperture and preservation of continuous wavefronts in the convergent beam after transmission through the structure

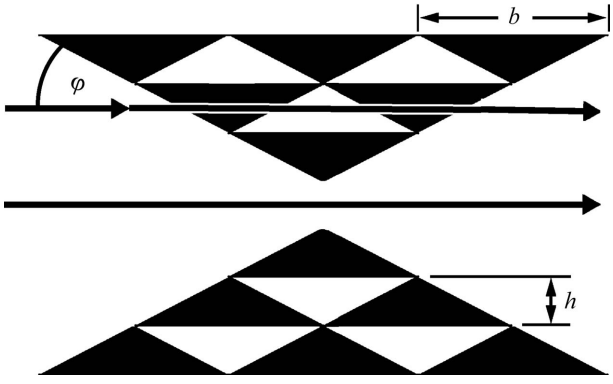

Figure 1
Cross section in the center of the clessidra lens, in which a large prism is composed of many smaller identical prisms with height h and base width b. The radiation beam travels along the arrows and hits the prism side-walls at an angle of grazing incidence φ.

(De Caro & Jark, 2008). The latter can be achieved in the longitudinally periodic radiation field for phase shifts accumulated in material, which are modulo 2π compared with travel in air. The corresponding material thickness B in the beam direction according to Suehiro *et al.* (1991) is

$$B = m\lambda/\delta, \tag{1}$$

where m is an integer ($m > 0$), λ is the wavelength of the incident radiation and δ is the real part of the refractive index decrement from unity of the lens material. The focusing is now a diffraction phenomenon and the related diffractive focal length for the highly periodic lens structure in Fig. 1 with periodicity h (prism height) is given by (Jark *et al.*, 2006)

$$f_{\rm dif} = \frac{h^2}{m\lambda}. \tag{2}$$

When the spatial coherence length is insufficient, *i.e.* no interference will occur between beams passing adjacent rows, then the image is produced by the refraction in the single rows. The beam deviation caused by the refraction in a symmetric prism is rather small and is given by (Cederström *et al.*, 2000) $\Delta = 2\delta/\tan\varphi$, where φ is the grazing angle between the beam trajectory and the prism side-walls. This leads to the common refractive focal length for all rows in the structure in Fig. 1 of

$$f_{\rm ref} = \frac{h}{\Delta} = \frac{h\tan\varphi}{2\delta}. \tag{3}$$

Obviously now the obtainable spatial resolution is limited by the height of the single rows to

$$r = c\frac{\lambda}{h}p. \quad (4)$$

The constant c depends on the exact boundary conditions and is of the order of 1.45 for a linear lens (Born & Wolf, 1980). The parameter p, which is $\geq f$, is the distance between the lens and the image plane. In clessidra lenses all rows provide the same maximum resolutions r, and technically feasible prisms will provide resolutions with $r \geq h$. Then even the use of straight prism side-walls will not deteriorate the image. The same also holds true for the diffraction-limited resolution in a spatially coherent beam for $m \leq 2$ as was shown by De Caro & Jark (2008). Consequently the curving of some prism side-walls as proposed by Jark *et al.* (2004) will not improve the obtainable spatial resolution, though it will improve the concentration of the radiation into a single diffraction peak (De Caro & Jark, 2008).

Where would be a typical application for these prism arrays? As far as aperture and focal length are concerned, a linear lens array cannot compete with the polycapillary lenses invented by Kumakhov (1990) for the beam concentration at laboratory X-ray sources. The micro-lens array is more suited for the beam properties at larger distances from synchrotron radiation sources; however, then for small source sizes s the illumination will still be spatially coherent at a source distance q in lines having lateral sizes (Attwood, 1999)

$$A_{\rm coh} = 0.44\frac{\lambda q}{s}. \quad (5)$$

$A_{\rm coh}$ and s refer here to the full width at half-maximum (FWHM) of the related properties. If we now require for incoherent illumination $A_{\rm coh} \leq h/2$, then we can identify appropriate operation conditions by use of equations (3) and (5) *via*

$$q \leq 2.3\, s\, \frac{\delta f}{\lambda \tan\varphi}. \quad (6)$$

It is advantageous to use longer focal lengths at larger sources and shorter wavelengths. These conditions were realised for the present experiment in order to test whether the many prisms in state-of-the-art clessidra lenses refract the incident beam compatibly with the above-described expectations.

2. Experimental details

Clessidras with larger prism heights are most adapted for this test and the parameters $h = 25.67$ µm, $b = 73.3$ µm and $\varphi = 35°$ were chosen. These lenses were produced lithographically (Pérennès *et al.*, 2005) into PMMA (polymethylmethacrylate) photoresist, which is $C_5H_8O_2$ with density 1.19 g cm^{-3}. The lens aperture in the focusing direction is 1.51 mm, and the etching in the orthogonal direction maintained the prism shape over a depth of 0.25–0.35 mm.

A long focal length is needed at the optics test beamline BM05 at the ESRF (http://www.esrf.eu/UsersAndScience/Experiments/Imaging/BM05/) when a refocusing lens and the detector are mounted at source distances of $q = 33$ m and of $q + p = 55$ m, respectively. The vertical electron beam size of $s = 83$ µm (BM05) can then be demagnified at the detector to an image size of $s' = sp/q = 55$ µm by any optical component having a focal length of $f = qp/(q + p) = 13.2$ m. The tabulation by Henke *et al.* (1993) for PMMA leads to $\delta = \delta_0(\lambda/\lambda_0)^2$ with $\delta_0 = 4.18 \times 10^{-6}$ at $\lambda_0 = 0.155$ nm (8 keV photon energy). According to equation (3), the present lens should refocus best a wavelength of $\lambda = 0.0626$ nm (19.8 keV photon energy). According to equations (6) and (1), this is achieved for incoherent illumination, when the expected phase discontinuities of modulo $0.8 \times 2\pi$ between the row borders are tolerable. In the experiment, a slit in front of the lens limited the illumination to the central 1.35 mm of the lens aperture to rows with $N \leq 26$ prisms.

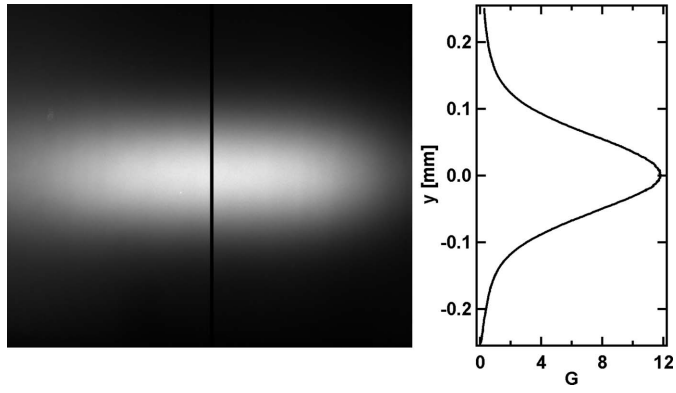

Figure 2
Left: CCD image of the intensity distribution in the image plane. The black line indicates where the vertical intensity distribution was quantitatively analysed as shown in the right-hand figure. No beam focusing is applied in the horizontal direction. The intensity variation in this direction is caused by the limited lens aperture in this direction of 0.25–0.35 mm and by an almost identical horizontal source size. Right: normalized vertical intensity distribution, *i.e.* gain G, averaged over 45 CCD columns in the flat center of the one-dimensionally focused beam (black line in the left-hand picture).

3. Experimental results and discussion

Fig. 2 shows the intensity distribution in the image plane registered by use of a high-resolution CCD camera with 0.645 µm equivalent pixel size and an exposure time of 20 s. As predicted, the smallest image size was found for 19.8 keV photon energy. Its measured FWHM size was about 125 µm, which is slightly larger than the expected image size[1] of $s' \simeq$ 110 µm. In agreement with ray-tracing calculations, a growth of the image size by 10% (12.5 µm) was observed when tuning the monochromator 110 eV away from the optimum setting. The flux integrated over twice the FWHM of the image size was about 65% of the incident flux, which leads to a measured maximum increase in photon flux density, *i.e.* in the gain G, of almost 12-fold.

The average transmission expected for a row with N prisms is $T = \exp[-(1/2)(Nb/L)]$. With an attenuation length of $L =$

[1] During the experiment the virtual source as seen from the detector position was moving aperiodically with frequencies in the Hz range. This was due to vibrations of unidentified origin in the beam transport system and lead in long time exposures ($t > 20$ s) to a virtual source size of approximately $s \simeq 170$ µm.

17 mm for PMMA at 19.8 keV photon energy (Henke *et al.*, 1993), this leads to $T = 0.945$ in the outermost row with $N = 26$. Thus the array with perfect prisms was supposed to refract almost 100% of the incident intensity into the image. However, it has been deduced already in independent experiments at 8.5 keV photon energy (Jark *et al.*, 2007) that 37% of the prism height in the more transparent tips refracted the beam far away from the common image position. The related reduction in the effective geometrical aperture of the prism rows to $h' = 0.63h = 16.2$ µm can then, according to (4), completely account for the measured image size. Thus, compared with the expectations for a perfect focusing optics under the same conditions, the tested lens provides a rather moderate performance deterioration with a growth in image size by 10% and a reduction in flux by 35%. Consequently the present prism array can already be a valid alternative to other optics for the beam concentration in this application.

We can now estimate the optimum aperture $A_{\rm opt}$ for such a micro-lens array, when we limit the average transmission in the outermost prism row containing $N_{\rm opt}$ prisms to $T = 0.5$. Then we find $N_{\rm opt} = 1.4L/b$ and $A_{\rm opt} = (2N_{\rm opt} + 1)h$, which by use of $\tan\varphi = 2h/b$ gives $A_{\rm opt} \simeq 1.4L\tan\varphi$.

With $L = 17$ mm (Henke *et al.*, 1993) for PMMA at 19.8 keV the present lens structure with $\tan\varphi = 0.7$ could thus be realised with the rather large aperture of $A_{\rm opt} \simeq L = 17$ mm, which is more than ten-fold the tested aperture.

It is very interesting to see that the present choice for q and p was also almost realised for the refocusing optics in another X-ray beamline. Shastri *et al.* (2007) report on the use of a silicon transmission lens for $q = 34$ m and $p = 22$ m with an aperture of 0.4 mm for a wavelength of $\lambda = 0.0153$ nm (81 keV photon energy). They already mention the possibility for an aperture increase by use of the clessidra design or its modification as introduced by Cederström *et al.* (2005). According to equation (5), the source size $s = 21$ µm leads to $A_{\rm coh} = 10.9$ µm. On the other hand, the prism heights required for clessidra operation in diffraction mode according to equation (2) are $h = 14.3$ µm for $m = 1$ and $h = 20.2$ µm for $m = 2$, respectively. Then the focusing could alternatively be performed with refractive micro-lens arrays with $h \geq 20$ µm. However, it is notable that these latter arrays will now provide at best image sizes $r \simeq h \simeq 20$ µm, which are slightly larger than the ideally demagnified source image of 14 µm.

For the prediction of the optimum aperture it is now more convenient to combine $A_{\rm opt} \simeq 1.4L\tan\varphi$ and equation (3) to give $A_{\rm opt} \simeq 2.8\delta L f_{\rm ref}/h$. Interestingly, for $E = 81$ keV the material property δL is almost identical for all materials with $Z < 14$ (Si), with $\delta L \simeq 1.5$ nm (Chantler *et al.*, 2003; Jark *et al.*, 2006). Then suitable clessidra prism arrays with easily feasible prism heights of $h \geq 20$ µm can be produced with similar apertures in a few lighter materials. For example, for $h = 20$ µm one would obtain an optimum aperture of $A_{\rm opt} = 2.84$ mm providing a seven-fold aperture increase compared with the presently operated standard transmission lens (Shastri *et al.*, 2007).

4. Conclusion

Is has been shown that state-of-the-art clessidra lenses can be used efficiently at longer focal length as arrays of purely refractive micro-lenses. The refraction efficiency within an aperture of 1.35 mm in the tested lens was 65%, which is consistent with the expectation considering already known defects in the prism tips. A rather significant aperture increase to $A_{\rm opt} = 17$ mm is possible under the present conditions for 20 keV photon energy. Another array could be optimized in a few materials as an efficient retrofit with seven-fold flux increase in an existing 81 keV X-ray beamline.

We are very grateful to A. Snigirev from ESRF for the help provided during the experiment.

References

Attwood, D. (1999). *Soft X-rays and Extreme Ultraviolet Radiation: Principles and Applications*, ch. 8. Cambridge University Press.
Born, M. & Wolf, E. (1980). *Principle of Optics*, 6th ed. New York: Pergamon.
Cederström, B., Cahn, R. N., Danielsson, M., Lundqvist, M. & Nygren, D. R. (2000). *Nature (London)*, **404**, 951.
Cederström, B., Ribbing, C. & Lundqvist, M. (2005). *J. Synchrotron Rad.* **12**, 340–344.
Chantler, C. T., Olsen, K., Dragoset, R. A., Kishore, A. R., Kotochigova, S. A. & Zucker, D. S. (2003). *X-ray Form Factor, Attenuation and Scattering Tables* (version 2.0), http://physics.nist.gov/ffast. [Originally published as Chantler, C. T. (2000). *J. Phys. Chem. Ref. Data*, **29**, 597–1048; and Chantler, C. T. (1995). *J. Phys. Chem. Ref. Data*, **24**, 71–643.]
De Caro, L. & Jark, W. (2008). *J. Synchrotron Rad.* **15**, 176–184.
Henke, B. L., Gullickson, E. M. & Davis, J. C. (1993). *Atom. Data Nucl. Data Tables*, **54**, 181–342. (http://www-cxro.lbl.gov/optical_constants/.)
Jark, W., Pérennès, F. & Matteucci, M. (2006). *J. Synchrotron Rad.* **13**, 239–252.
Jark, W., Perennes, F., Matteucci, M., Mancini, L., Menk, R. H. & Rigon, L. (2007). *AIP Conf. Proc.* **879**, 796–799.
Jark, W., Pérennès, F., Matteucci, M., Mancini, L., Montanari, F., Rigon, L., Tromba, G., Somogyi, A., Tucoulou, R. & Bohic, S. (2004). *J. Synchrotron Rad.* **11**, 248–253.
Kumakhov, M. A. (1990). *Nucl. Instrum. Methods*, **48**, 283–286.
Lesem, L. B., Hirsch, P. M. & Jordan, J. A. Jr (1969). *IBM J. Res. Dev.* **13**, 150–155.
Pérennès, F., Matteucci, M., Jark, W. & Marmiroli, B. (2005). *Microelectron. Eng.* **78–79**, 79–87.
Shastri, S. D., Almer, J., Ribbing, C. & Cederström, B. (2007). *J. Synchrotron Rad.* **14**, 204–211.
Suehiro, S., Miyaji, H. & Hayashi, H. (1991). *Nature (London)*, **352**, 385–386.
Yang, B. X. (1993). *Nucl. Instrum. Methods*, A**328**, 578–587.